Proc. Natl. Acad. Sci. USA
Vol. 89, pp. 10213–10217, November 1992
Biochemistry

Acid-induced structural changes in human rhinovirus 14: Possible role in uncoating

VINCENT L. GIRANDA*†, BEVERLY A. HEINZ‡§, MARCOS A. OLIVEIRA*, IWONA MINOR*, KYUNG HYUN KIM*, PRASANNA R. KOLATKAR*, MICHAEL G. ROSSMANN*¶, AND ROLAND R. RUECKERT‡

*Department of Biological Sciences, Purdue University, West Lafayette, IN 47907; and ‡Institute for Molecular Virology, University of Wisconsin, Madison, WI 53706.

Contributed by Michael G. Rossmann, July 20, 1992

ABSTRACT **X-ray diffraction data were collected from human rhinovirus 14 crystals a few minutes after exposure to acid vapor and prior to excessive crystalline disorder. Conformational changes occurred (*i*) in the GH loop of viral protein (VP) 1, (*ii*) at the ion binding site on the outer surface of the pentamer center, and (*iii*) in VP3 and VP4 on the virion's interior in the vicinity of the fivefold axis. Amino acid substitutions in mutants resistant to low pH, or to drugs that inhibit uncoating, were concentrated in the vicinity of the GH loop. It is proposed that the acid-induced changes reflect processes that trigger uncoating.**

The genus *Rhinovirus* is composed of a group of over 100 serologically distinct viruses, which are a major cause of the common cold in humans (1). These viruses belong to the picornavirus family, which also contains the genera *Enterovirus, Aphthovirus*, and *Cardiovirus*. The picornaviruses are small, icosahedral, nonenveloped, single-stranded RNA viruses. X-ray crystal structures have been determined for at least one member in each picornavirus genus (2–7). Polioviruses (genus *Enterovirus*) are structurally the most similar to rhinoviruses. Unlike the enteroviruses, the rhinoviruses are unstable below pH 6.

Each of the 60 icosahedral protomers in picornaviruses contains four viral polypeptides, VP1–VP4. VP1, VP2, and VP3 reside on the exterior of the virus and make up its protein shell (Fig. 1). These three peptides contain a common eight-stranded antiparallel β-barrel motif. Their amino termini intertwine to form a network on the interior of the protein shell. Five VP3 amino termini form a five-stranded, helical β-cylinder on the virion's interior about each icosahedral fivefold axis. This β-cylinder stabilizes the pentamer and is thought to be important for its assembly (3, 8).

VP4 is smaller than the other viral polypeptides and resides inside the virion's protein shell. The amino terminus of VP4 is myristoylated and may help the association of VP4 with the lipid membrane bilayer during viral uncoating or assembly (9). In poliovirus the myristoylate moiety lies inside the virion coat close to the β-cylinder. The first 25–28 amino-terminal residues of VP4 are disordered in the rhinovirus structures, but a density consistent with myristoylate is seen internally near the center of the pentamer in rhinoviruses 14 and 1A (6, 10) (Fig. 1*B*). In poliovirus the amino terminus of VP4 is ordered and forms two strands of a three-stranded β-sheet. The third strand of the sheet is donated by residues of the amino terminus of VP1 (5).

Productive viral uncoating requires that the RNA move from inside the viral protein shell, through a cellular membrane, into the cytosol. Such displacement requires large conformational changes in the rhinovirus coat. For poliovirus or rhinovirus, the acidification of the endosomes is thought to be required for an infection to proceed normally as measured by either progeny virus production or cytopathic effects (11–14), although this hypothesis is not yet universally accepted (15).

The 149S native virus particles are thought to uncoat (Fig. 2) through intermediate 125S particles (16, 17), which are similar to the "A particles" formed *in vitro* by exposure of rhinoviruses to acid (18). The A particles can also be formed in the absence of acid but in the presence of cells (refs. 11 and 15; D. A. Shepard and R.R.R., unpublished results) or soluble receptor (19). The cellular receptor of the major group of rhinoviruses (20) is intercellular adhesion molecule 1 (21, 22). Mutational (23–25) and structural (N. H. Olson, P.R.K., M.A.O., R. H. Cheng, J. M. Greve, A. McClelland, T. S. Baker, and M.G.R., unpublished results) studies support the idea that intercellular adhesion molecule 1 interacts with the GH loop at the bottom of the canyon (Fig. 1). The A particles still contain RNA, but have lost VP4, and are no longer infectious. It has been shown for poliovirus that formation of the 125S particle is coupled to the externalization of the amino terminus of VP1 (26). The externalized VP1 amino terminus may convey the ability of this particle to associate with lipid bilayers.

Inhibition of uncoating of rhinoviruses *in vivo* can be caused by lipophilic compounds binding in a hydrophobic pocket inside VP1 (27). In some serotypes these compounds also inhibit attachment (28, 29). These uncoating inhibitors fill up a normally vacant region underneath the GH loop of VP1 (corresponding to the most antigenic sequence in foot-and-mouth disease virus) that forms a portion of the canyon floor (Fig. 1). In rhinovirus 14 this GH loop must be displaced to permit the pocket to accommodate these inhibitors (30–33). These drugs have also been shown to stabilize the virus to acidification (34) and heat (27) *in vitro*. Stabilization of VP1 has been invoked as the mechanism of inhibition of uncoating for these compounds (30). The structural changes upon acidification of wild-type rhinovirus 14 will be discussed here and correlated with data from a number of acid-resistant mutants (ref. 35 and this manuscript) as well as with data from a number of mutants (24) that are resistant to uncoating inhibitors.

EXPERIMENTAL PROCEDURES

Wild-type plaques of human rhinovirus 14 (HRV14) were individually amplified at 35°C for 8 hr in monolayer HeLa cell cultures to increase the number of resistant viruses they contained and to unmask viral mosaics that had formed during plaque formation (28). To isolate acid-stable mutants,

The publication costs of this article were defrayed in part by page charge payment. This article must therefore be hereby marked "*advertisement*" in accordance with 18 U.S.C. §1734 solely to indicate this fact.

Abbreviations: HRV14, human rhinovirus 14; VP, viral protein.

†Present address: Therapeutic Center, Eastman Kodak Co., Rochester, NY 14650-2158.
§Present address: Lilly Research Laboratories, Virology Research, Lilly Corporate Center, Indianapolis, IN 46285.
¶To whom reprint requests should be addressed.

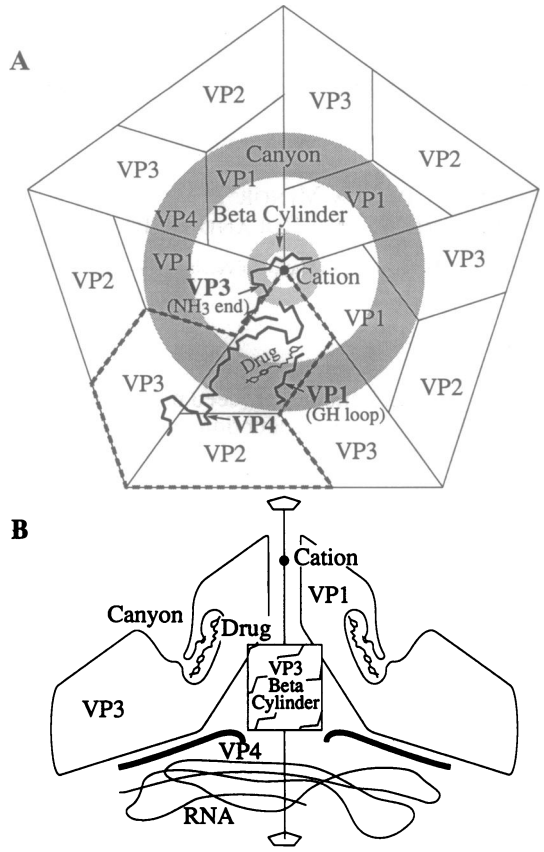

FIG. 1. (*A*) Schematic representation of 1 of 12 pentamers in the protein shell of rhinovirus 14. A single cation, probably Ca^{2+}, is located at the center on the outer surface. The large shaded region is the canyon, a 25-Å-deep depression on the surface of the virus, encircling the fivefold axis. The bold lines indicate structural features (GH loop in VP1 residues 217–225, VP3 residues 1–20, VP4 residues 29–65) belonging to one protomer (dashed outline), which may be important in the uncoating process. VP4, located on the interior surface of the protomer, has its amino end near the β-cylinder (small shaded region). The β-cylinder (see also *B*) spans the interior third of the capsid and is composed of five pentamerically related amino ends of VP3 encircling the fivefold axis. The GH loop of VP1 forms part of the floor of the canyon and also the ceiling of the drug binding pocket. (*B*) Cross-section containing the fivefold axis showing some of the above features.

about 10^7 plaque-forming units of each amplified wild-type preparation were diluted 10-fold into 10 mM citrate buffer containing 0.4% bovine serum albumin (final pH of 4.5) for 5 min at room temperature and neutralized by 10-fold dilution into phosphate-buffered saline containing 0.4% bovine serum albumin. Virus suspensions were inoculated onto cells and allowed to produce plaques in agar. Independent acid-stable and drug-resistant mutants (Table 1) were isolated as described (24). Immunoprecipitation, extraction, and sequencing were performed as described by Heinz *et al.* (28).

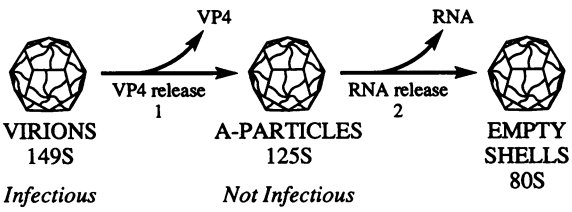

FIG. 2. Two steps in the uncoating of picornaviruses. The first step, release of VP4, is mediated by interaction with viral receptor, by decreasing pH, or by heating to 52°C. The second step, release of RNA, may be caused by acidification of the membrane-bound particle.

Table 1. Rhinovirus 14 mutations

Phenotype	Mutations in VP1
Acid resistant	H78L, H78Y, N100K, N100T, D101E, N145S, W163R, V188A, V191A, T216I, M221L, M224L, A225V
Drug resistant	N100S, N105S, V153I, N219S, S223G

The mutation designations are as follows: the wild-type amino acid residue (single-letter code) and its position number are given followed by the amino acid replacing it. For example, H78L indicates a mutation where histidine at residue 78 was replaced by leucine.

Rhinovirus 14 crystals were acidified through the vapor phase by sealing them in a capillary with Tris·HCl buffer plus glacial acetic acid at a final concentration of 10%. Within 15 min, the crystals had changed from clear to yellow and no longer could diffract x-rays. In contrast, crystals sealed in capillaries without volatile acid could last at least 24 hr with no ill effects. Data were collected immediately after addition of acid to the capillary in a series of 0.3° oscillation photographs, which were exposed for 30–50 sec, using the intense x-ray beam (wavelength of 0.91 Å) now available at the F1 station of the Cornell High Energy Synchrotron Source. The data (Table 2) were processed according to established procedures (36) and divided into two sets in order to determine if the magnitude of changes was related to the length of time that the crystals had been exposed to acid. Electron density difference maps with Fourier coefficients of $(2|F_{acid}| - |F_{neutral}|)$ and $(|F_{acid}| - |F_{neutral}|)$ were calculated using native rhinovirus 14 phases.

RESULTS AND DISCUSSION

Three areas in the rhinovirus structure were disordered on acidification: the ion binding site at the icosahedral fivefold axis (10), the interior of the virus shell near the fivefold axis, and the GH loop of VP1 (Fig. 3). Furthermore, the magnitude of the disorder increased as the time of acid exposure increased (Table 3).

The large negative intensity on the difference map indicates that, upon acidification, there is loss of the cation (10) that is coordinated to the carbonyl oxygens of Asn-141 of five VP1s (Fig. 3*A*). This result is reminiscent of the ion loss in tomato bushy stunt virus (37, 38) and southern bean mosaic virus (39) uncoating, albeit the ions are not in analogous locations. Loss of the cation in certain drug-resistant mutants of HRV14 (Table 3) is accompanied by movement of the DE loop, which contains the coordinating carbonyls of Asn-141, thereby slightly expanding the pore channel down the fivefold axis. The maps of acidified HRV14 suggest a similar change of the DE loop, but the results are not conclusive.

Table 2. HRV14 data processing of acidified wild type

Parameter	Data set		
	All	Early†	Late‡
Crystals	11	4	8
Films	60	12	20
Resolution, Å	2.9	2.9	2.9
Total reflections	630,434	148,097	203,530
Unique reflections	366,040	130,047	164,140
% total observed	58.0	20.6	26.0
R^*_{sym}	14.7	13.3	14.4

$R^*_{sym} = [\Sigma_h \Sigma_i |\langle I_h \rangle - I_{hi}| / \Sigma_h \Sigma_i \langle I_h \rangle] \times 100$, where I_h is the mean of the i intensities I_{hi} for reflection h.

†Early data were collected between 0 and 6 min after exposure to acid vapor.

‡Late data were collected after 7 min of exposure to acid vapor.

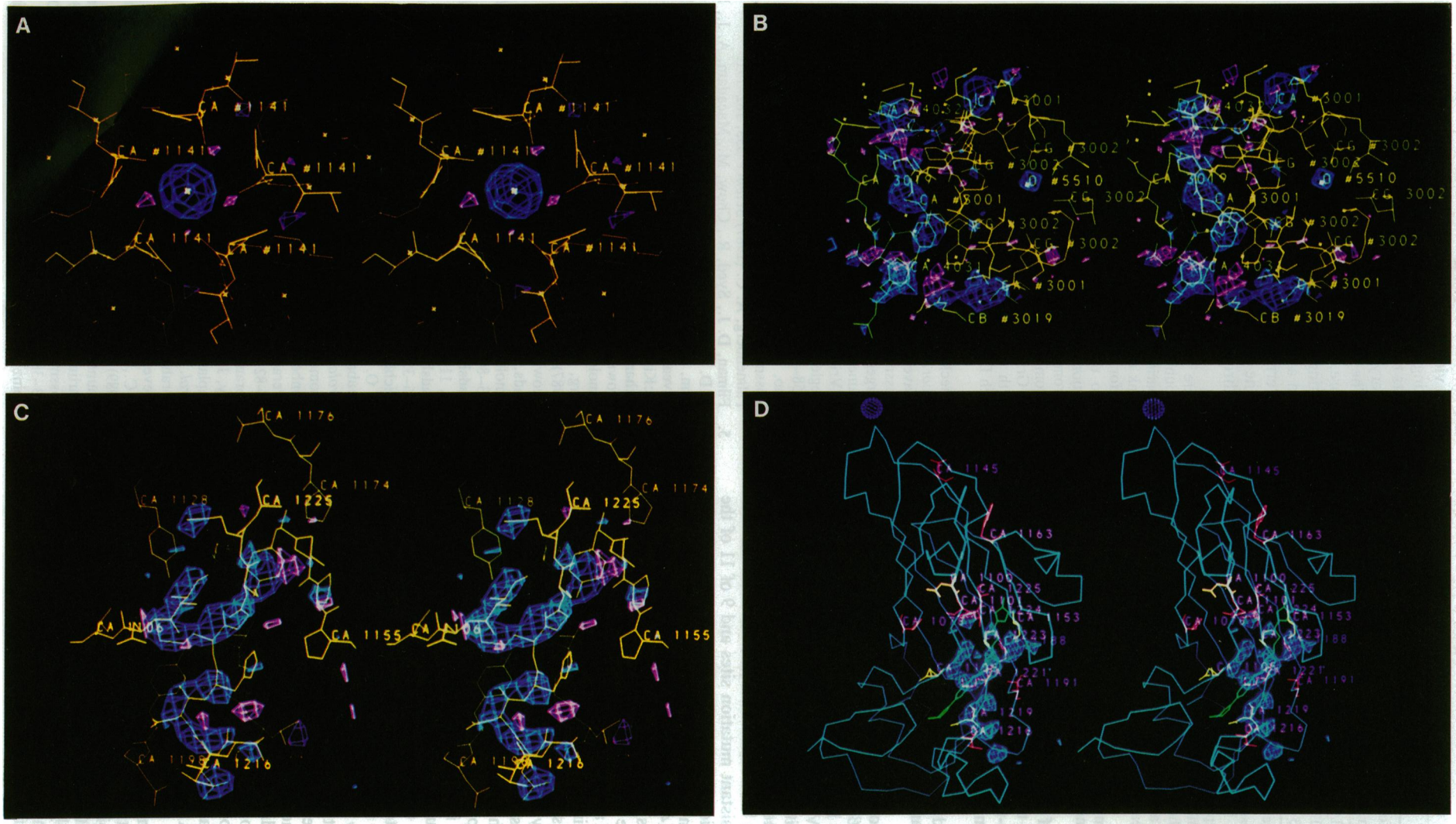

FIG. 3. (*A–C*) Stereoviews of regions of rhinovirus 14 that become disordered on acidification. The virus structure is depicted in yellow. Blue baskets depict negative areas on $|F_{acid}| - |F_{neutral}|$ difference maps and are indicative of disorder. Pink baskets depict regions of positive density on difference maps. All views are roughly from outside the virus looking inward. The first digit of each residue number corresponds to the viral peptide. (*A*) Loss of the cation at the fivefold axis. (*B*) Disorder of the amino termini of VP3 and VP4 in the region of the β-cylinder. The water atom O #5510 lies on the icosahedral fivefold axis near the interior of the virus coat. (*C*) Disorder in the GH loop and flanking regions of VP1. Some additional residue identifications have been added to orient the viewer. (*D*) Proximity of the acid-resistant (red) and virus inhibitor-resistant (yellow) mutation sites (Table 1) to the region of disorder (blue baskets) in the GH loop of VP1. The α-carbon backbone of VP1 is depicted in blue. The position of the hydrophobic pocket is indicated by the model of a bound viral inhibitor (green). The fivefold cation is shown as a violet sphere. The view is looking into the canyon.

Table 3. Changes on rhinovirus 14 acidification

Data set	Maximum absolute magnitude			
	Fivefold ion	VP4	GH loop	L17V mutant
All	81	45	36	100
Early*	51	39	33	100
Late†	123	54	42	100

The values given are the maximum absolute magnitudes of peak heights on ($|F_{acid}| - |F_{neutral}|$) difference maps. All peaks are negative in the difference maps. Maps are normalized with respect to the peak caused by the phenotypically silent mutation L17V, which occurs in all rhinovirus maps since 1986. The largest noise peak is about 26 units with respect to the L17V mutation peak in all cases. The data show that in the three areas of disorder, the magnitude with respect to the L17V mutant peak increases with the time of exposure of the crystal to acid.
*Soaking time of <6 min.
†Soaking time of >7 min.

Another region of disorder is also near each icosahedral fivefold axis, but on the interior of the viral coat. This region contains the amino-terminal myristoylate of VP4 and the five-stranded β-cylinder formed by the VP3 amino termini. Residues 29–39 of VP4 become disordered as does the amino-terminal residue of VP3 (Fig. 3*B*). This disorder may reflect structural changes that precede release of VP4 to form A particles.

Finally, the GH loop becomes disordered between residues 215 and 223. The β-strands, on the floor of the canyon, adjacent to the GH loop also show disordering at residues 103, 104, and 154 in VP1. All three strands are in contact with the uncoating inhibitor binding site and correspond to the regions that have the largest conformational changes when uncoating inhibitors bind inside VP1 (30, 31).

Five of 5 drug-resistant mutation sites and 9 of 11 of the acid-resistant mutation sites are in or immediately surround the disordered region about the GH loop (Fig. 3*D*). Of the two exceptions, one (N145S) is near the fivefold axis cation and the other (W163R) is on a protomer interface. The mutation sites described here for rhinovirus 14 have little exposed surface area (23) and are well ordered. This is true for mutants that affect stability in other proteins (40–42). Changes that add hydrogen bonds or salt bridges to a protein normally increase its stability (43). Mutations that reduce mobility around the mutated site (e.g., a smaller to a larger residue or replacing linear with branched-chain residues) are also expected to increase protein stability. Four of five inhibitor-resistant mutations in HRV14 are changes from larger to smaller residues, thus likely to be destabilizing. Nine of 13 acid-stable mutants (Table 1) are changes from smaller to larger or from linear to branched residues and, thus, are likely to be stabilizing. In two of the acid-resistant mutant structures, some density is visible in the hydrophobic pocket within VP1, suggesting that a cellular cofactor may have bound in the pocket, thereby stabilizing the virion in a manner similar to the uncoating inhibitors (5, 30).

In summary, acidification of human rhinovirus crystals disorders three regions: the fivefold cation site, the β-cylinder, and the GH loop of VP1. Disorder in VP4 may represent initial conformational changes preceding its ejection during the formation of A particles. Mutations conferring drug resistance and acid stability are predominantly in the GH loop region. The combination of (*i*) the acid-induced disorder of the GH loop, (*ii*) the enhanced stabilization by binding of the uncoating inhibitors close to the GH loop, (*iii*) the acid-stabilizing effect on the virion of mutations in the region of the GH loop (Table 1) (35), (*iv*) the destabilizing effect of mutations conferring resistance to uncoating inhibitors (counteracting that of the binding of the inhibitor compounds) in the vicinity of the GH loop, and (*v*) the initiation of uncoating by the binding of the receptor to the canyon suggests that the conformational changes in the GH loop are necessary for the uncoating process leading to the release of VP4. The expansion of the β-cylinder and cation release may, therefore, be among the first events during this process, permitting eventually the escape of VP4s, possibly along fivefold axis channels. There are parallels to this process in the externalization of VP1 through the fivefold axis channel of canine parvovirus (44) and the ejection of single-stranded DNA through the fivefold ion channel of φX174 (45).

We are grateful to Dieter Blaas for sending us his manuscript before publication (35) and to Marcia Kremer and Grazyna Apostol for preparing many of the crystals on which these studies were based. We thank the whole staff of the Cornell High Energy Synchrotron Source for their help and interest in making these studies possible. We also thank Helene Prongay and Sharon Wilder for help in preparation of the manuscript. This work was supported by Grant AI 27310 from the National Institutes of Health to M.G.R., Grant AI 24939 from the National Institutes of Health to R.R.R., postdoctoral training Grant CA09075 in viral oncology from the National Institutes of Health to B.A.H., and the Sterling-Winthrop Pharmaceuticals Research Division.

1. Rueckert, R. R. (1990) in *Fundamental Virology, 2nd Edition. Picornaviridae and Their Replication*, ed. Fields, B. N. (Raven, New York), pp. 357–390.
2. Rossmann, M. G., Arnold, E., Erickson, J. W., Frankenberger, E. A., Griffith, J. P., Hecht, H. J., Johnson, J. E., Kamer, G., Luo, M., Mosser, A., Rueckert, R. R., Sherry, B. & Vriend, G. (1985) *Nature (London)* **317**, 145–153.
3. Hogle, J. M., Chow, M. & Filman, D. J. (1985) *Science* **229**, 1358–1365.
4. Luo, M., Vriend, G., Kamer, G., Minor, I., Arnold, E., Rossmann, M. G., Boege, U., Scraba, D. G., Duke, G. M. & Palmenberg, A. C. (1987) *Science* **235**, 182–191.
5. Filman, D. J., Syed, R., Chow, M., Macadam, A. J., Minor, P. D. & Hogle, J. M. (1989) *EMBO J.* **8**, 1567–1579.
6. Kim, S., Smith, T. J., Chapman, M. S., Rossmann, M. G., Pevear, D. C., Dutko, F. J., Felock, P. J., Diana, G. D. & McKinlay, M. A. (1989) *J. Mol. Biol.* **210**, 91–111.
7. Acharya, R., Fry, E., Stuart, D., Fox, G., Rowlands, D. & Brown, F. (1989) *Nature (London)* **337**, 709–716.
8. Arnold, E., Luo, M., Vriend, G., Rossmann, M. G., Palmenberg, A. C., Parks, G. D., Nicklin, M. J. H. & Wimmer, E. (1987) *Proc. Natl. Acad. Sci. USA* **84**, 21–25.
9. Chow, M., Newman, J. F. E., Filman, D., Hogle, J. M., Rowlands, D. J. & Brown, F. (1987) *Nature (London)* **327**, 482–486.
10. Arnold, E. & Rossmann, M. G. (1990) *J. Mol. Biol.* **211**, 763–801.
11. Madshus, I. H., Olsnes, S. & Sandvig, K. (1984) *J. Cell Biol.* **98**, 1194–1200.
12. Madshus, I. H., Olsnes, S. & Sandvig, K. (1984) *Virology* **139**, 346–357.
13. Zeichhardt, H., Wetz, K., Willingmann, P. & Habermehl, K. O. (1985) *J. Gen. Virol.* **66**, 483–492.
14. Neubauer, C., Frasel, L., Kuechler, E. & Blaas, D. (1987) *Virology* **158**, 255–258.
15. Gromeier, M. & Wetz, K. (1990) *J. Virol.* **64**, 3590–3597.
16. Lonberg-Holm, K. & Korant, B. D. (1972) *J. Virol.* **9**, 29–40.
17. Everaert, L., Vrusen, R. & Boeye, A. (1989) *Virology* **171**, 76–82.
18. Korant, B. D., Lonberg-Holm, K., Yin, F. H. & Noble-Harvey, J. (1975) *Virology* **63**, 384–394.
19. Kaplan, G., Freistadt, M. S. & Racaniello, V. R. (1990) *J. Virol.* **64**, 4697–4702.
20. Abraham, G. & Colonno, R. J. (1984) *J. Virol.* **51**, 340–345.
21. Greve, J. M., Davis, G., Meyer, A. M., Forte, C. P., Yost, S. C., Marlor, C. W., Kamarck, M. E. & McClelland, A. (1989) *Cell* **56**, 839–847.
22. Staunton, D. E., Merluzzi, V. J., Rothlein, R., Barton, R., Marlin, S. D. & Springer, T. A. (1989) *Cell* **56**, 849–853.
23. Rossmann, M. G. & Palmenberg, A. C. (1988) *Virology* **164**, 373–382.
24. Heinz, B. A., Shepard, D. A. & Rueckert, R. R. (1990) in *Use*

of X-ray Crystallography in Design of Antiviral Agents, eds. Laver, W. G. & Air, G. M. (Academic, San Diego), pp. 173–186.
25. Colonno, R. J., Condra, J. H., Mizutani, S., Callahan, P. L., Davies, M. E. & Murcko, M. A. (1988) *Proc. Natl. Acad. Sci. USA* **85**, 5449–5453.
26. Fricks, C. E. & Hogle, J. M. (1990) *J. Virol.* **64**, 1934–1945.
27. Fox, M. P., Otto, M. J. & McKinlay, M. A. (1986) *Antimicrob. Agents Chemother.* **30**, 110–116.
28. Heinz, B. A., Rueckert, R. R., Shepard, D. A., Dutko, F. J., McKinlay, M. A., Fancher, M., Rossmann, M. G., Badger, J. & Smith, T. J. (1989) *J. Virol.* **63**, 2476–2485.
29. Pevear, D. C., Fancher, M. J., Felock, P. J., Rossmann, M. G., Miller, M. S., Diana, G., Treasurywala, A. M., McKinlay, M. A. & Dutko, F. J. (1989) *J. Virol.* **63**, 2002–2007.
30. Smith, T. J., Kremer, M. J., Luo, M., Vriend, G., Arnold, E., Kamer, G., Rossmann, M. G., McKinlay, M. A., Diana, G. D. & Otto, M. J. (1986) *Science* **233**, 1286–1293.
31. Badger, J., Minor, I., Kremer, M. J., Oliveira, M. A., Smith, T. J., Griffith, J. P., Guerin, D. M. A., Krishnaswamy, S., Luo, M., Rossmann, M. G., McKinlay, M. A., Diana, G. D., Dutko, F. J., Fancher, M., Rueckert, R. R. & Heinz, B. A. (1988) *Proc. Natl. Acad. Sci. USA* **85**, 3304–3308.
32. Chapman, M. S., Giranda, V. L. & Rossmann, M. G. (1990) *Sem. Virol.* **1**, 413–427.
33. Chapman, M. S., Minor, I., Rossmann, M. G., Diana, G. D. & Andries, K. (1991) *J. Mol. Biol.* **217**, 455–463.
34. Gruenberger, M., Pevear, D., Diana, G. D., Kuechler, E. & Blaas, D. (1991) *J. Gen. Virol.* **72**, 431–433.
35. Skern, T., Torgersen, H., Auer, H., Kuechler, E. & Blaas, D. (1991) *Virology* **183**, 757–763.
36. Rossmann, M. G. (1985) *Methods Enzymol.* **114**, 237–280.
37. Robinson, I. K. & Harrison, S. C. (1982) *Nature (London)* **297**, 563–568.
38. Hogle, J. M., Kirchhausen, T. & Harrison, S. C. (1983) *J. Mol. Biol.* **171**, 95–100.
39. Abdel-Meguid, S. S., Yamane, T., Fukuyama, K. & Rossmann, M. G. (1981) *Virology* **114**, 81–85.
40. Alber, T., Dao-pin, S., Nye, J. A., Muchmore, D. C. & Matthews, B. A. (1987) *Biochemistry* **26**, 3754–3758.
41. Matthews, B. A. (1987) *Biochemistry* **26**, 6885–6888.
42. Argos, P., Rossmann, M. G., Grau, U. M., Zuber, H., Frank, G. & Tratschin, J. D. (1979) *Biochemistry* **18**, 5698–5703.
43. Perutz, M. F. & Raidt, H. (1975) *Nature (London)* **255**, 256–259.
44. Tsao, J., Chapman, M. S., Agbandje, M., Keller, W., Smith, K., Wu, H., Luo, M., Smith, T. J., Rossmann, M. G., Compans, R. W. & Parrish, C. R. (1991) *Science* **251**, 1456–1464.
45. McKenna, R., Xia, D., Willingmann, P., Ilag, L. L., Krishnaswamy, S., Rossmann, M. G., Olson, N. H., Baker, T. S. & Incardona, N. L. (1992) *Nature (London)* **355**, 137–143.